α,α-Trehalose-Water Solutions VI. A View of the Structural and Dynamical Properties of Oβ*G* Micelles in the Presence of Trehalose

S. Magazù,*,† V. Villari,‡ A. Faraone,† G. Maisano,† R. K. Heenan,§ and S. King§

Dipartimento di Fisica and INFM dell'Università di Messina, C.da Papardo S.ta Sperone 31, 98166 Messina, Italy, Istituto per i Processi Chimico-Fisici, Sezione di Messina-CNR, Via La Farina 237, 98123 Messina, Italy, and ISIS Facility, Rutherford Appleton Laboratory, Chilton, Didcot, OX11 OQX, United Kingdom

Received: March 13, 2002

The protective effect of trehalose on biological membranes against freezing or dehydration has been the subject of many studies aimed at understanding the reasons of the effectiveness of this disaccharide under environmental stress conditions, and the trehalose−water interaction mechanisms. This work reports on the results of a study on the octyl-β-glucoside/trehalose/water ternary solution, performed by Small-Angle Neutron Scattering and Photon Correlation Spectroscopy, to show the effect of the presence of trehalose on the dynamical and conformational properties of the octyl-β-glucoside (Oβ*G*) micelles. The evolution of the micelles' size and shape, as well as of the hydrodynamic radius with the increase of trehalose amount have been determined using these techniques. The data suggest that the trehalose−water interaction is preferred in the investigated concentration range.

Introduction

The preservation of biological molecules during the freeze-drying and lyophilization processes, widely employed in the pharmaceutical, medical, and food industries has considerably evolved in recent decades. Sugars have been frequently employed for protecting both proteins and cells during these procedures. The most promising saccharide, which displays the highest effectiveness in protecting biomembranes, is trehalose ($C_{12}H_{22}O_{11}$), a disaccharide of glucose. Trehalose is particularly effective in preserving and maintaining the activity and functionality of several desiccation-resistant organisms,[1−4] which are able to survive without water for decades and, in some cases, centuries; they rapidly resume their metabolism, frequently within minutes, when rehydrated.[3,5,6] A common feature in these organisms is the synthesis, induced by heat shock, of a large amount of trehalose. Until now, many studies have been devoted to analyzing the thermoactivation and thermoprotective action of sugars on enzymes,[7] liposomes[8] as well as on isolated biological membranes or proteins,[7−11] but it emerged that the other disaccharides induce only a partial stabilization when compared with trehalose. For example, the membranes may also be stabilized in the dry state by lyophilizing them in sucrose, but a higher amount (about three times more) is required.[12]

Many different mechanisms have been proposed to account for the peculiarities of trehalose: its ability to form glass at a higher temperature than that of the other disaccharides[13,14] or to interact strongly with water and lipid membranes, just to cite the main ones.[15,16]

On the basis of the peculiar properties of trehalose, a series of experimental studies have been performed by our group, focusing attention on the molecular point of view.[17−21] Although the bioprotective effectiveness of disaccharides reflects a complex array of interactions at the structural, physiological, and molecular levels, it appears that interactions that derive from the unique properties of the water molecules are involved.

A comparison between different disaccharides performed by quasi-elastic neutron scattering[21] evidenced that although the dynamics of the three homologous disaccharides are not very different, except perhaps for the inter-ring mobility (higher for trehalose), and although the population of water molecules in the primary hydration shell is quite similar, in the case of trehalose/H_2O solutions the dynamics of water is sensitively slowed not only in respect to the bulk water, but also to water in the other disaccharides.

As far as the direct interaction with proteins is concerned, a lot of work has been devoted to the study of the effect of trehalose on proteins' function and dynamics. Gottfried et al.[22] showed that trehalose, in a protein/trehalose/water mixture in the glassy state, interacting more strongly with the protein than water does, directly couples the heme to the complex network-linked solvent molecules that form the glass. The absence of substantial conformational effects in a trehalose-embedded protein (hemoglobin) suggested that the different behavior, in the presence of trehalose, could be connected with changes in protein dynamics. Cordone et al.,[11,23] moreover, found that trehalose coating prevents thermal denaturation by damping large-scale fluctuations of protein specific motions that could cause protein unfolding. It has been shown in a work by Allison et al.[24] that the degree of structural protection conferred by trehalose correlates with the extent of hydrogen bonding between sugar and protein; this bonding is necessary to prevent dehydration-induced protein damage. In our recent work by photon correlation spectroscopy,[19] we simulated the interaction of trehalose with proteins, studying the ternary solution poly(ethylene oxide)/trehalose/water as a function of concentration and temperature. The chemical structure of the polymer, simpler

† Dipartimento di Fisica and INFM dell'Università di Messina.
‡ Istituto per i Processi Chimico-Fisici, Sezione di Messina-CNR.
§ ISIS Facility, Rutherford Appleton Laboratory.

10.1021/jp020698y CCC: $22.00
Published on Web 06/17/2002

than that of proteins, and its helical conformation in water, which mimes the primary, secondary and tertiary protein structure, constitute a useful starting point in the understanding of the more complex protein/trehalose/water interactions. The work gave experimental evidence that interactions (direct or mediated by water) of trehalose with polymer coils exist only at high trehalose content and affect the diffusive polymer dynamics and the coil conformational properties with temperature. On the basis of these findings, it is possible to infer that also in the case of proteins, trehalose could affect the protein structural properties, stabilizing the swelling and collapsing effect connected with temperature and, hence, obstructing thermal degradation.

A thorough examination in this direction is reported in the present paper, which involves a study of another ternary solution: octyl-β-glucoside/trehalose/water. Octyl-β-glucoside (OβG) ($C_{14}H_{28}O_6$), is a nonionic surfactant, constituted by a glucose head and a hydrophobic alkyl tail (with eight CH_2 groups); it is widely employed in the fractionation and reconstitution of components of biological membranes. It was introduced for membrane studies by Baron and Thomson[25] and it is now used because of its ability to solubilize water-insoluble proteins from membranes without denaturation and to maintain the activity of membrane enzymes dispersed in aqueous solutions. Above the critical micellar concentration (cmc = 0.025 *m*, where *m* is the molality) OβG molecules aggregate in water forming ellipsoidal micelles whose gyration radius is about 28 Å at $T = 25$ °C. The cmc depends on temperature, but, in the range investigated in the present paper, between 25 °C and 60 °C, it keeps constant. This amphiphilic molecule has been studied deeply to determine its thermodynamic properties;[26] cmc, size, aggregation number and micelle molar mass have been investigated a lot in the past, but few studies have been performed to investigate the micellar properties' dependence on concentration and temperature. Although this molecule is a non-ionic surfactant, the presence of hydroxyl groups in the glucose ring promotes the interaction with water and is responsible for the main differences with other non-ionic surfactants. This occurrence, together with the fact that OβG micelles could mime small lipid layers, suggested to us the choice of this ternary system. The aim of the present work, in fact, is to study the micelles' dynamics in water and to determine the effect of the increased amount of trehalose on the dynamical and conformational properties of the micelles themselves, using Small-Angle Neutron Scattering (SANS) and Photon Correlation Spectroscopy (PCS).

Samples and Experimental Setup. As far as SANS measurements are concerned, an octyl-β-glucoside/D_2O solution, at a concentration of 0.1m (m stands for molality), was prepared dissolving a weighted amount of surfactant, purchased from Fluka, in ultrapure heavy water. Ternary systems containing trehalose, purchased from Aldrich-Chemie, were prepared dissolving OβG and trehalose in D_2O. Five samples were prepared corresponding to trehalose/OβG molar ratios, *R*, equal to 0.28, 0.57, 1.43, 3.45, and 4.35. Great care was taken to obtain stable, clear and dust-free samples. SANS data were collected on the LOQ instrument at ISIS facility (DRAL, UK).[27] Samples were held in quartz spectrophotometric cells (path length 2 mm) and mounted in a thermostat which stabilizes temperatures within ±0.2 °C. The diffractometer worked at 25 Hz with an incident wavelength, λ, of 2.2−10 Å ($\Delta\lambda/\lambda \cong 5\%$), and a sample−detector distance of 4.05m; with this setup the accessible range of momentum transfer ($4\pi(\theta/2)]/\lambda$, θ being the scattering angle) is 0.008−0.25 Å^{-1}. In all cases the two-dimensional scattering contours, corrected for detector efficiency, instrumental background etc., were isotropic. Therefore, they were reduced to 1D radial averages and then converted to scattering cross sections per unit volume (cm^{-1}) using a polymer sample as standard secondary calibration by the program COLETTE.[28,29]

For the light scattering measurements, binary (OβG/H_2O) and tertiary (OβG/trehalose/H_2O) solutions were prepared weighting a certain amount of solute in pure distilled light water. The OβG/H_2O solutions were investigated in the concentration range 0.066÷2 m, determining the diffusion coefficient evolution with concentration and temperature. Then, having chosen the OβG concentration value of 0.1 m in respect to water (low enough to neglect both intermicellar interaction and monomer contribution), the ternary systems were prepared varying the molar ratio, *R*, between trehalose and OβG molecules (in practice, only the amount of trehalose was increased). All the systems were carefully subordinated to a filtering procedure in recirculation with an Amicon Millipore filter 0.2 μm of diameter pore size, to obtain autocorrelation functions with good signal-to-noise ratio and without dust.

Quasielastic Light Scattering measurements were performed by means of PCS technique, using a standard scattering apparatus described in detail elsewhere.[17,19] As exciting source, the 4880 Å vertically polarized line of an Ar^+ laser was used. Samples were mounted in a thermostat with a temperature control better than ±0.02 °C and the temperature range was between 25 °C and 60 °C.

Data Analysis. From a general point of view the experimentally determined quantity in a diffraction experiment is the diffraction cross section, namely the collected scattered neutrons for each scattering angle θ, without performing any energy analysis.[30] The diffraction signal is thus the sum of a coherent term containing the structural information superimposed on a flat (apart from a Debye−Waller factor) incoherent term. To enhance the signal-to-noise ratio, the incoherent contribution is reduced using deuterated samples.

In a SANS experiment, the neutron wavelength is of the order of a few Å and its energy of a few meV. Under these conditions, the scattering event can be considered elastic, and $Q = 4\pi/\lambda \sin(\theta/2)$. Small *Q* experiments ($|Q| < 1$ Å^{-1}) are actually small angle scattering experiments (scattering angles less than about 100 mrad).[31] Taking into account the sizes in colloidal systems, for example a micellar solution, it can be deduced that SANS is very often the more appropriate technique for the study of their structure.

In the case of a solution of monodisperse and centrosymmetric particles, under the hypothesis of independence of intermolecular and intramolecular averages, the coherent differential scattering cross section can be factorized in the product of three terms[32]

$$\left(\frac{d\sigma}{d\Omega}\right)_{\mathrm{coh}} = nP(Q)S(Q) \qquad (1)$$

where *n* is the number density, *P(Q)* is the form factor and *S(Q)* is the structure factor. When interactions can be neglected, for example in very diluted solutions, the static structure factor is equal to unity and the scattering cross section is proportional to the form factor

$$\left(\frac{d\sigma}{d\Omega}\right)_{\mathrm{coh}} = nP(Q) = |\int_V (\rho - \rho_{\mathrm{solv}}) \exp(iQ\cdot r)dV|^2 = nK^2V^2f(Q) \qquad (2)$$

where the integral is on the volume of the particle V, ρ, and ρ_{solv} are the coherent scattering length densities of the particle and solvent respectively, $K = \rho - \rho_{solv}$ is the contrast, and $f(Q)$ is a function that takes into account the shape of the particle ($f(Q = 0) = 1$).

As far as the light scattering measurements are concerned, we used the Photon Correlation Spectroscopy technique.[33,34] It allows measurement of the correlation function of the scattered intensity $I_S(Q,t)$

$$G_2(Q,t) = \langle I_S(Q,0) I_S(Q,t) \rangle \tag{3}$$

If the scattered field obeys the Gaussian statistics, the Siegert's relationship can be applied

$$G_2(Q,t) = \langle I(Q) \rangle^2 [1 + \alpha |G_1(Q,t)|^2] \tag{4}$$

where α is a constant which depends on the experimental setup and $G_1(Q,t)$ is the field autocorrelation function. In the time domain typical for a light scattering experiment ($\geq 10^{-6}$ s), that is for times between the characteristic viscous flow relaxation and the diffusive relaxation over a scale as great as particle dimension, hydrodynamic interactions can be considered as instantaneous and direct interactions do not affect particle configuration.[35,36] Under these conditions and for diffusing monodisperse spherical scatterers, intensity correlation function decays exponentially, according to

$$G_2(t) = \langle I(Q) \rangle^2 [1 + \alpha \exp(-2 D_c Q^2 t)] \tag{5}$$

In the limit $Q \rightarrow 0$, the effective diffusion coefficient is identified with the collective diffusion coefficient, defined by the generalized Stokes−Einstein relation $D_c = (\partial \Pi / \partial c)_T \, 1/\zeta(c) \, (1 - \upsilon c)$, with $(\partial c / \partial \Pi)_T \propto [S(0)]^{-1}$ osmotic compressibility, ζ frictional coefficient, υ molecule partial specific volume and c the concentration. The concentration dependence of D_c gives information about intermolecular interactions; in the dilute regime, in fact, the first-order virial expansion can be applied

$$D_c = D_0 (1 + k_D c) \tag{6}$$

The sign and magnitude of the slope, k_D, are related, neglecting the contribution of the volume υ, to frictional and osmotic compressibility virial coefficients, and, hence, to the character of direct and frictional interactions[37]

$$k_D = 2A_2 M - B_\zeta \tag{7}$$

with A_2 and B_ζ the second virial coefficient of direct and frictional interactions, respectively.

In the very diluted limit, the theory of Brownian motion relates the measured D to the self-diffusion coefficient D_0, which is connected to the center of mass motion of the isolated scatterer and allows the evaluation of the hydrodynamic radius, R_H, of the particles by the Einstein-Stokes (ES) relation

$$D_0 = \frac{K_B T}{6 \pi \eta R_H} \tag{8}$$

where η is the viscosity coefficient of the continuous medium.[33]

Whereas for the analysis of OβG/water systems the autocorrelation function decay is exponential, the addition of trehalose stretches the functions; consequently, in such a case for the normalized first-order autocorrelation function, the Kohlraush−Williams−Watt (KWW) function is more suitable[38,39]

$$g_1(t) = A \exp\left[- \left(\frac{t}{\tau_{KWW}} \right)^{\beta_{KWW}} \right] \tag{9}$$

where β_{KWW}, which ranges from 0 to 1, is the shape parameter measuring the broadening of the relaxation time distribution. The average diffusive relaxation time is related to τ_{KWW} by: $\langle \tau \rangle = (\tau_{KWW}/\beta_{KWW}) \Gamma(1/\beta_{KWW})$, with $\Gamma(x)$ the gamma function.

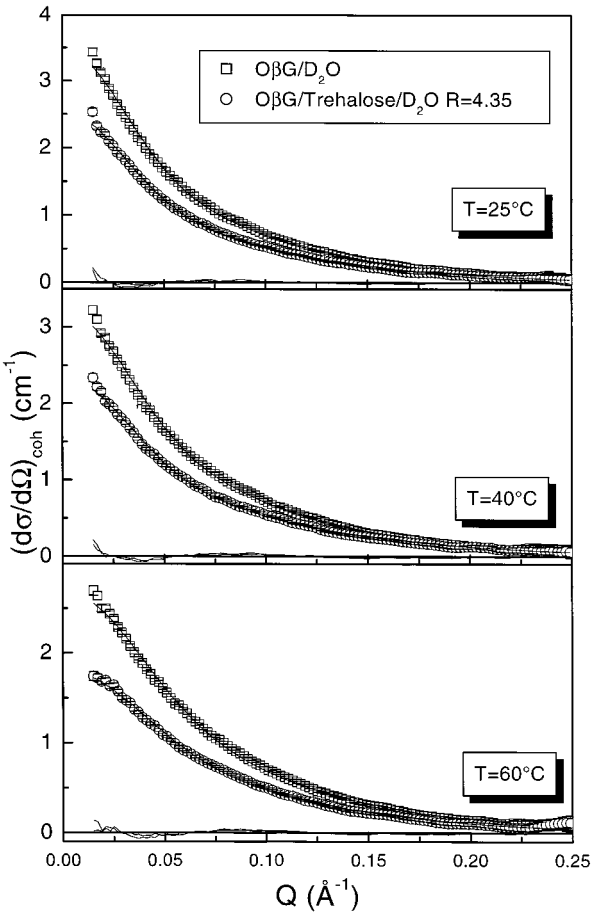

Figure 1. Scattered intensities from OβG/D_2O and OβG/trehalose/D_2O ($R = 4.35$) solutions at different temperature values. Continuous lines are the fit according to eq 2. The residuals are also reported.

Results and Discussion

The SANS spectra of the OβG/D_2O sample, at the concentration $c = 0.1$ m, and of the OβG/trehalose/D_2O ternary solution corresponding to the highest trehalose content ($R = 4.35$) are shown in Figure 1 for the three investigated temperatures.

For analyzing the SANS spectra of the ternary solutions, we consider that, at the concentration value of 0.1 m, the intermicellar interactions, and hence the effects of the structure factor, can be neglected. This assumption is supported by the findings reported in ref 40, in which it was found that interparticle interactions can be neglected for concentration values up to $c = 0.15$ m.

As can be seen in Figure 1, the low-Q intensity decreases as the trehalose content increases. This finding can be rationalized considering that trehalose dissolved in water changes the scattering length density of the solvent, with a net diminishing of the contrast K.

On the basis of a previous work[40] we analyzed our data using a model that assigns to the OβG micelles a form factor of an ellipsoid having semiaxes a, a, and $c = Ba$, where B is the ratio between the two axes. The case $B = 1$ trivially corresponds to a sphere, while the $B < 1$ and $B > 1$ cases indicate oblate and prolate ellipsoids, respectively.[40] The radius of gyration, R_g, is related to the shape parameters a and c through the formula[41]

$$R_g^2 = \frac{1}{5}(2a^2 + c^2) \tag{10}$$

where the radius of gyration is defined by the equation

$$R_g^2 = \frac{\int r^2[\rho(r) - \rho_0]d^3r}{\int [\rho(r) - \rho_0]d^3r} \tag{11}$$

The coherent scattering cross section, in such a case, can be written as

$$\left(\frac{d\sigma}{d\Omega}\right)_{coh} = nK^2[V(a,c)]^2 \int_0^1 [3j_1(u)/u]^2 d\mu = I(0)\int_0^1 [3j_1(u)/u]^2 d\mu \tag{12}$$

where n is the number concentration of the micelles, $u(\mu)$ is defined as $u(\mu) = Qa[B^2\mu^2+(1-\mu^2)]^{1/2}$ (μ being the cosine of the angle between the directions of c and Q), $j_1(u)$ is the first-order spherical Bessel function, and the contrast is $K=\rho_{O\beta G}-\rho_{solv}$. The scattering length density of OβG is

$$\rho_{O\beta G} = \frac{N_A}{M_{O\beta G}} d_{O\beta G}[14b_C + 28b_H + 6b_O] = 4.29 \cdot 10^9 \text{cm}^{-2} \tag{13}$$

where $d_{O\beta G}$ and $M_{O\beta G}$ are the density and the molecular weight of OβG, and N_A is Avogadro's Number.

In Figure 1, the continuous lines are the fits according to eq 12. For the OβG/D_2O binary solution the value of the small semiaxis a is constant (~11 Å) with temperature, whereas the semiaxis c decreases as T increases, because of thermodynamic effects, taking the values 73 Å at 25 °C, 67.3 Å at 40 °C, and 57.3 Å at 60 °C (the corresponding R_g values obtained by using relation (10) are 33.4 Å at 25 °C, 30.9 Å at 40 °C and 26.6 Å at 60 °C). These findings are in agreement with previous measurements on OβG aqueous solutions[40] and suggest two considerations: (i) because the size of the OβG molecule is about 18.5 Å,[26] some interpenetration of the alkyl chains within the micelles takes place; (ii) the micelles appear like cylinders whose dimensions are mainly determined by the value of the long semiaxis c.

As far as the dependence on the trehalose/OβG molar ratio is concerned, in Figure 2a we show the values of both the semiaxes as a function of R at the different temperatures. Neither of the semiaxes depends on trehalose amount. However, because the $I(0)$ values depend on the contrast factor, the addition of trehalose results in a change in the low-Q intensity according to the trehalose arrangement in solution.

Assuming that trehalose is completely dissolved in water and is not present in the micelles, it is possible to evaluate the aggregation number, N_{aggr}, of the micelles. The scattering length density of OβG is given by eq 13. The evaluation of the scattering length density of the solvent requires the consideration that the non-aggregated monomer concentration in the aqueous phase is cmc = 0.025 m. Because the D_2O/OβG molar ratio

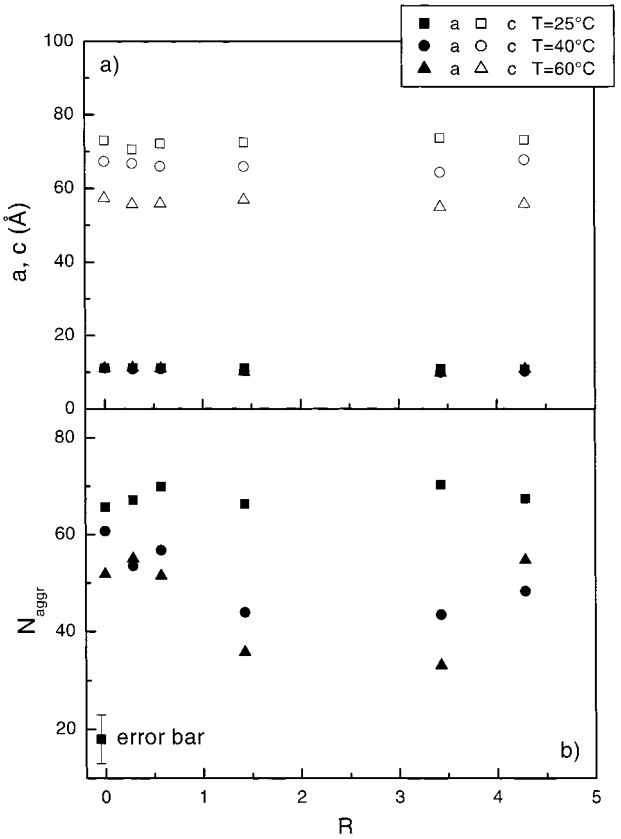

Figure 2. (a) Micellar geometric parameters, a and c, plotted as a function of the trehalose amount at T = 25, 40, and 60 °C. (b) Aggregation number of OβG micelle plotted versus trehalose/OβG molar ratio.

corresponding to c = 0.1m is 500, it results that 0.225 OβG molecules per 500 D_2O molecules are present in the aqueous phase. We have

$$\rho_{solv} = \frac{N_A}{M_{solv}} d_{solv}\left[500b_{D_2O} + 0.225b_{O\beta G} + \frac{1}{R}b_{trehalose}\right]$$
$$M_{solv} = \left[500M_{D_2O} + 0.225M_{O\beta G} + \frac{1}{R}M_{trehalose}\right] \tag{14}$$

where b_α and M_α are the scattering length and molecular mass of α particle. The density values, d_{solv}, used for calculating ρ_{solv} are reported in ref 42.

The aggregation number can now be straightforwardly calculated from the relation

$$I(0) = nK^2[V(a,c)]^2 = \frac{(c_{O\beta G} - c_{cmc})N_A}{N_{aggr}M_{O\beta G}}[\rho_{O\beta G} - \rho_{solv}]^2\left[\frac{4}{3}\pi a^2 c\right]^2 \tag{15}$$

where $I(0)$ is expressed in absolute units (cm^{-1}), the concentration in gr/cm^3 and V(a,c) is the micelle's volume. Once a and c are determined through the fit, it is possible to determine the aggregation number, N_{aggr}, from eq 15. Alternatively, instead of using eq 13, it is possible to write the micelle scattering length density as

$$\rho_{O\beta G} = \frac{N_{aggr}}{V}[14b_C + 28b_H + 6b_O] \tag{16}$$

Combining equations 15 and 16 we get a second-order equation

for N_{aggr}. The values of N_{aggr} obtained solving this equation have been reported in Figure 2b). They are in very good agreement with those obtained calculating $\rho_{O\beta G}$ from eq 13. The aggregation number decreases as trehalose increases, especially at $T =$ 40 and 60 °C for OβG/trehalose molar ratios equal to 0.70 and 0.29. Dividing the surface, $S = 2\pi\{a^2+\theta[a^3\cdot(c^2 - a^2)^{-1/2}+ a\cdot(c^2 - a^2)^{1/2}]\}$ (with $\theta = \arcsin[(1 - a^2/c^2)^{1/2}]$) and volume, $V(a,c) = 4\pi a^2 c/3$, of the OβG micelles by N_{aggr}, the surface ($\sim$120 Å^2) and volume ($\sim$600 Å^3) per head are obtained. These values for the trehalose-free system and their trend for the OβG/trehalose/water mixture are in fairly good agreement with the results obtained by Teixeira et al.[40] for the OβG/water and OβG/Glycine/water solutions.

The circumstance that the aggregation number decreases with increasing temperature in the case of the trehalose-free system corresponds to a decrease in the micellar size (c varies from 73 Å at 25 °C to 57 Å at 60 °C). On the other hand, whereas at $T =$ 20 °C, N_{aggr} keeps constant, at $T =$ 40 °C and $T =$ 60 °C, there is a decrease of N_{aggr} as the trehalose amount increases, without substantial changes in the semiaxes' values. As a consequence, the volume and surface per head slightly increase with the trehalose content. This result can be rationalized by hypothesizing that although most trehalose molecules are in dispersed in water (as suggested by the decrease in $I(0)$), a small number of trehalose molecules can interact with micelles or with the water molecules of the hydration layer.

Once the structural properties were evaluated from the SANS results, we performed Photon Correlation Spectroscopy measurements on the binary and ternary solutions in order to characterize the dynamics of the micelles.

The decay rate, Γ, of the autocorrelation functions, and its Q^2-dependence, allowed us to extract the diffusion coefficient values. From the whole evolution of the collective diffusion coefficient of the OβG micelles in water, reported in Figure 3a), as a function of micelles' concentration (c-cmc), it is possible to deduce the intermicellar interaction character and the micelles' size. The notation "c-cmc" takes into account that a certain amount of monomer (equal to cmc) is present in the nonaggregated form. At micelles' concentration values up to 0.975 m, the solutions show very low polydispersity values and the analysis using both the single and the stretched exponential furnishes the same results. Below 0.125 m, the increased polydispersity can be due to the fact that near the cmc, the scattered intensity from micelles is comparable with that from the single molecules. This could also be the reason why the diffusion coefficient rapidly increases below this concentration value.

The initial decrease of D_c can be interpreted with the presence of intermicellar attractive interactions; the minimum and the following increase show a balance between attraction and steric repulsion, the latter being predominant at higher concentrations. The plateau between 0.5 and 0.8 m confirms that the initial decrease of D_c is not simply due to the hydrodynamic hindrance, which increases with the volume fraction of the disperse phase. A sight of the scattered intensities as a function of micelles' concentration, shown in Figure 3b), confirms what emerged from the D_c evolution. It is in good qualitative agreement with the theoretical hard sphere model, according to which the minimum and maximum observed respectively in the diffusion coefficient and in the intensity are related to the system osmotic compressibility[35,36] with a perturbation due to a small additional contribution in the interaction potential (see, for example: ref 43). This reproduces attractive and repulsive (hard core) interactions at low concentration, and the dominant repulsive interactions at high concentration.

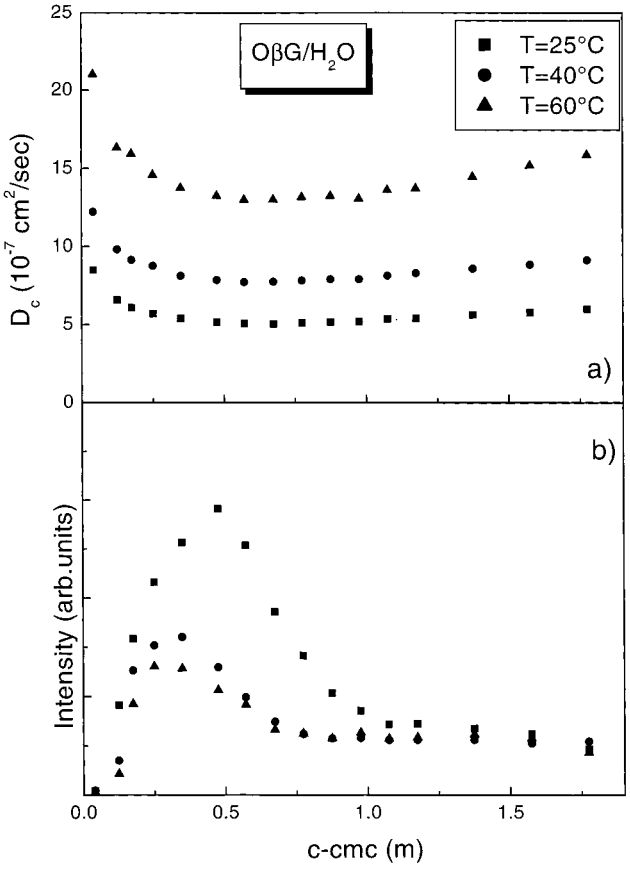

Figure 3. (a) Concentration dependence of the micellar collective diffusion coefficient for three different temperature values. (b) Scattered intensity from the OβG aqueous solutions at different temperature values.

TABLE 1: Fit Parameters Obtained by Using Relation 8

	25 °C	40 °C	60 °C
D_0 (10^{-7} cm^2/sec)	9.1	13.0	22.3
R_H (Å)	26.9	27.1	23.4
k_D (10^7)	−5.5	−4.8	−5.1

The intensity evolution as a function of concentration, moreover, shows that the maximum is at $\sim$0.5m (volume fraction $\approx$ 0.1) for $T =$ 25 °C, defining an overlapping region beyond which the micellar occupied volumes touch each other.

A comparison with the SANS results supports such conclusions; the form factor gives a gyration radius of about 30 Å. From a geometric calculus of rotation volumes, the concentration at which the ellipsoids start to touch is 0.4 ÷ 0.5 m; this value corresponds to the plateau of the diffusion coefficient. Moreover, the extrapolation of the structure factor of SANS measurements, by Teixeira et al., at zero angle,[40] whose value is related to the second virial coefficient, furnished a negative value at low concentration, namely the presence of attractive interaction as found from the present light scattering results.

Using the relation 6 in the dilute regime (below 0.25 m) one obtains the extrapolation of the diffusion coefficient, D_0, and the k_D values; they are reported in Table 1 together with the hydrodynamic radii evaluated by the Einstein−Stokes relation 8. Figure 4 reports the R_H evolution with temperature and the corresponding values for the most dilute solution (c-cmc = 0.041); such a comparison provides for a quantitative estimation of the effect of the extrapolation procedure on the R_H value. The fact that at concentration values lower than $c =$ 0.1m, R_H is slightly smaller than R_g (evaluated by SANS) can be attributed

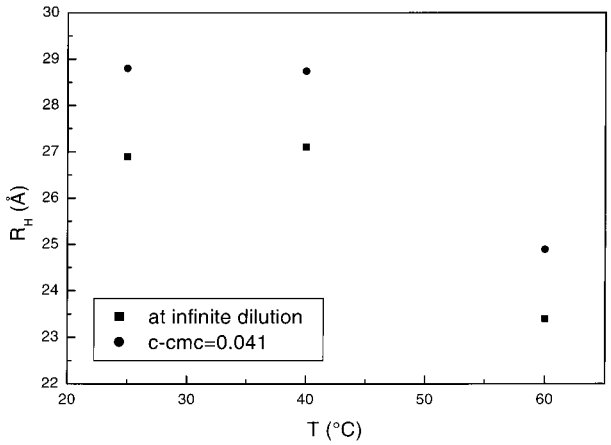

Figure 4. Hydrodynamic radius evaluated from the relation 8 as a function of temperature.

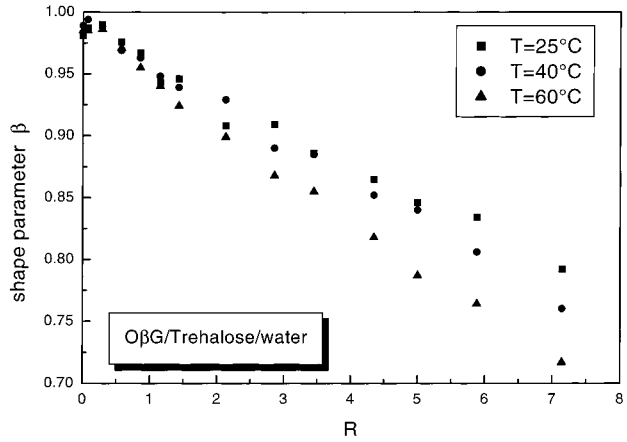

Figure 5. Shape parameter evolution of the stretched exponential for the ternary solutions as a function of the trehalose/OβG molar ratio.

to the presence of weak (van der Waals) interactions between micelles, as already discussed. SANS experiments, in fact, need a solute amount high enough to ensure a good signal-to-noise ratio and reliability. The two sets of values keep constant in the range from 25 °C to 40 °C and decrease at $T = 60$ °C (however, calculating the hydrodynamic radius at $c = 0.1$ m, we found that $R_H = 32.8$ Å at $T = 25$ °C, $R_H = 31.2$ Å at $T = 40$ °C, and $R_H = 27.5$ Å at $T = 60$ °C, in perfect agreement with the R_g values).

Once the dynamical properties of OβG micelles have been characterized, it is possible to extract information on the effects induced by the addition of trehalose on the micellar dynamics. Because the light scattered intensity scales with the square of the particle mass, the scattering from a micelle is about 60^2 times that of a single trehalose molecule, because the surfactant and the disaccharide have roughly the same molecular weight and the micelle is composed of ~60 OβG molecules. This means that the dynamics of micelles will dominate; even at the highest trehalose concentration the contribution due to the micelle is estimated to be ~7 times that of the disaccharide.

The stretching of the autocorrelation functions of the ternary system starts to become significant only at a trehalose/OβG molar ratio equal to $R = 3.45$, even though the shape parameter β keeps values always above 0.7 (see Figure 5). Also in the case of the ternary systems, therefore, from the Q scanning of the decay rate of the correlation functions, we can extract a single (mean) diffusion coefficient representing the micelles' diffusion. The extracted OβG micellar diffusion coefficient values, reported as a function of R, are shown in Figure 6.

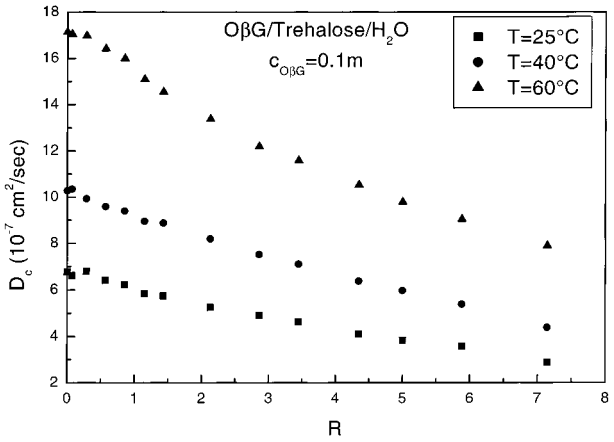

Figure 6. Micellar collective diffusion coefficient as a function of the trehalose/OβG molar ratio.

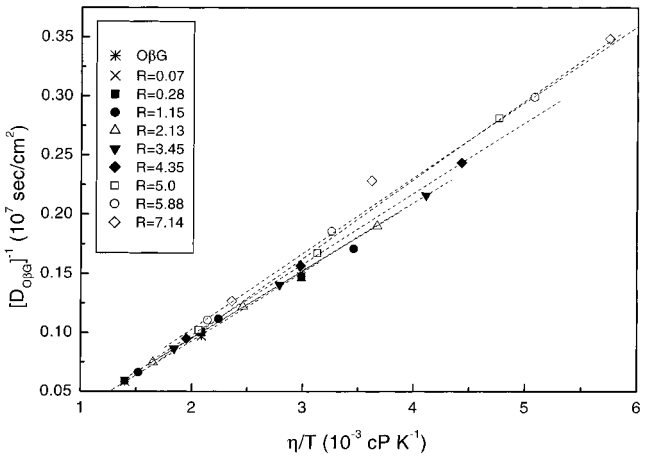

Figure 7. Viscosity-scaled plot of the micellar diffusive behavior for different trehalose amounts.

Starting from the values corresponding to the trehalose-free system, they decrease, indicating that increasing the trehalose amount slows down the diffusive behavior of the micelles.

Under the hypothesis that at $c = 0.1$ m the intermicellar interactions are weak enough to be neglected, from the calculation of the hydrodrynamic radius simply using the viscosity values of water, we found that R_H trivially increases with the trehalose amount. Therefore, reporting D^{-1} as a function of η/T (η being the viscosity of the trehalose in water mixture, reported in refs 17 and 19) at different trehalose concentration values (see Figure 7), the effect of the increased viscosity is taken into account. As it clearly appears in the figure, up to $R = 4.35$, the hydrodynamic radius, evaluated from the slope of the data behavior, keeps constant to the value corresponding to the trehalose-free system. This occurrence indicates that at low concentration, OβG and trehalose seem not to interact with each other. For this evaluation the T-dependence of the micellar size at higher temperature, already in evidence, has been neglected. Above $R = 4.35$ an increase in R_H becomes evident (up to about 44 Å).

Conclusion

From the SANS results, it emerges that the micelles' size does not depend on the trehalose amount, whereas the aggregation number decreases as the disaccharide amount increases. At low trehalose content the geometric parameters of the micelles are comparable with those of the trehalose-free system; when trehalose concentration in respect to water is higher than

4% w/w ($R \approx 1.4$), the aggregation number decreases especially at $T = 40$ °C and $T = 60$ °C, although the semiaxes' values remain constant. This occurrence could be rationalized considering that, although most trehalose molecules are dissolved in water, some fraction of trehalose can be present in the micelle's shell. The PCS data, on the other hand, furnish a complementary picture, suggesting that when the diffusion coefficient is properly scaled for the viscosity of the trehalose/water mixture, the hydrodynamic radius of the micelles is not affected by the presence of trehalose up to a trehalose/OβG molar ratio of $R = 4.35$. Above this value an increase in R_H occurs. Comparing the information obtained from the two techniques, we can deduce that at lower concentration values trehalose interacts more with water molecules than with micelles without modifying the structure of the micellar system substantially. These findings suggest that, at low concentration, the protective action of trehalose is not connected to a direct interaction with the membranes (in this case, schematically modeled by the OβG micelles), and it is more likely mediated through the interaction with water.[20,44,45] At higher concentrations, both the geometric modifications of the micelles and the increase of R_H can be the sign of the presence of interactions between trehalose molecules and micelles: some trehalose molecules could be present in the shell of the micelle, inserted between the OβG glucose heads or linked to the fraction of water molecules of the hydration layer.

References and Notes

(1) Li, J. C. *J. Chem Phys.* **1996**, *105*, 6733.

(2) Bourne, Y.; Cambillau, C. *Topics Mol. Biol.* **1993**, *17*, 321.

(3) Leslie, S. B.; Israeli, E.; Lighthart, B.; Crowe, J. H.; Crowe, L. M. *Appl. Environ. Microbiol.* **1995**, *61*, 3592.

(4) Clegg, J. S. *Comp. Biochem. Physiol*. **1967**, *20*, 8.

(5) Elbein, A. D. *Chem. Biochem.* **1974**, *30*, 227.

(6) Sussman, A. S.; Halvorson, H. O. *Spores: Their Dormancy and Germination*; Harper & Row: New York, 1966.

(7) Carnici, P. *Biochemistry* **1998**, *95*, 520.

(8) Sun, W. Q.; Leopold, L. M.; Crowe, L. M.; Crowe, J. H. *Biophys. J.* **1996**, *70*, 1769.

(9) Hottiger, T.; De Virgilio, C.; Hall, M. N.; Boller, T.; Wiemken, A. *Eur. J. Biochem.* **1994**, *219*, 187.

(10) Crowe, J. H.; Carpenter, J. F.; Crowe, L. M. *Annu. Rev. Physiol.* **1998**, *60*, 73.

(11) Cordone, L.; Ferrant, M.; Vitrano, E.; Zaccai, G. *Biophys. J.* **1999**, *76*, 1043.

(12) Crowe, J. H.; Crowe, L. M.; Jackson, S. A. *Arch. Biochem. Biophys.* **1983**, *220*, 477.

(13) Angell, C. A. *Science* **1995**, *267*, 1924.

(14) Green, J. L.; Angell, C. A. *J. Phys. Chem.* **1989**, *93*, 2880.

(15) Crowe, J. H.; Crowe, L. M.; Chapman, D. *Science* **1984**, *223*, 701.

(16) Crowe, J. H.; Crowe, L. M. *Biological Membranes*; Chapman, D., Ed.; Academic Press: New York, 1984, 57.

(17) Magazù, S.; Maisano, G.; Middendorf, H. D.; Migliardo, P.; Musolino, A. M.; Villari, V. *J. Phys. Chem. B* **1998**, *102*, 2060.

(18) Magazù, S.; Maisano, G.; Migliardo, P.; Tettamanti, E.; Villari, V. *Molecular Physics* **1999**, *96*, 381.

(19) Magazù, S.; Maisano, G.; Migliardo, P.; Villari, V. *J. Chem. Phys.* **1999**, *111*, 9086.

(20) Branca, C.; Magazù, S.; Maisano, G.; Migliardo, P.; Villari, V.; Sokolov, A. P. *J. Phys.: Condens. Matter* **1999**, *11*, 3823.

(21) Magazù, S.; Villari, V.; Migliardo, P.; Maisano, G.; Telling, M. T. F. *J. Phys. Chem.* **2001**, 105, 1851.

(22) Gottfried, S. D.; Peterson, E. S.; Sheikh, A. G.; Wang, J.; Yang, M.; Friedman, J. M. *J. Phys. Chem.* **1996**, *100*, 12 034.

(23) Cordone, L.; Galajda, P.; Vitrano, E.; Gassmann, A.; Ostermann, A.; Parak, F. *Eur. Biophys. J. Biophys. Lett.* **1998**, *27*, 173.

(24) Allison, S. D.; Chang; B.; Randolph, T. W.; Carpenter, J. F. *Arch. Biochem. Biophys.* **1999**, *365* (2), 289.

(25) Baron, C.; Thompson, T. E. *Biochim. Biophys. Acta* **1975**, *382*, 276.

(26) Kameyama, K.; Takagi, T. *J. Colloid Interface Sci.* **1990**, *137*, 1.

(27) Heenan, R. K.; King, S. M. *Proceedings of the International Seminar on Structural Investigations at Pulsed Neutron Sources*; Aksenovon, V. L., Balagurov, A. M., Taran Yu, V., Eds.; Publication E3-93-65, JINR. Dubna 1993.

(28) Heenan, R. K.; Penfold, J.; King, S. M. *J. Appl. Crystallogr.* **1997**, *30*, 1140.

(29) Gilbert, R. J. C.; Heenan, R. K.; Timmins, P. A.; Gingles, N. A.; Mitchell, T. J.; Rowe, A. J.; Rossjohn, J.; Parker, M. W.; Andrew, P. W.; Byron, O. *J. Mol. Biol.* **1999**, *293*, 1145.

(30) Volino, F.; Dianoux, A. J. "New Developments in Neutron Scattering for the Study of Molecular Systems: Structure and Diffusive Motions" In. *Proceedings of the Euchem. Conf. 'Organic Liquids; Structures Dynamics and Chemical Properties'*; John Wiley and Sons Ltd.: New York, *17*, 1978.

(31) Caponetti, E.; Triolo, R. *Adv. Coll. Inter. Sci.* **1990**, *32*, 235.

(32) Teixeira, J. Introduction to Small Angle Neutron Scattering Applied to Colloidal Science. In. *Structure and Dynamics of Strongly Interacting Supramolecular Aggregates in Solution*; S.-H. Chen et al., Eds.; Kluwer Academic Publishers: Norwell, MA, 1992.

(33) Berne, B. J.; Pecora, R. *Dynamic Light Scattering with Application to Chemistry, Biology and Physics*; J. Wiley & Sons: New York, 1976.

(34) Cummins, H. Z. Light Beating Spectroscopy. In. *Photon Correlation and Light Beating Spectroscopy*; Cummins, H. Z., Pike, E. R. Plenum Press: New York, 1974.

(35) Klein, R.; Nägele, G. *Il Nuovo Cimento* **1994**, *16*, 963.

(36) Pusey, P. N.; Tough, R. J. A. In. *Dynamic Light Scattering: Application of Photon Correlation Spectroscopy*; Berne, B. J., Ed.; Plenum Press: New York, *85*, 1985.

(37) Brown, W.; Nicolai, T. *Dynamic Light Scattering. The Method and Some Applications*; Brown, W., Ed.; Clarendon: Oxford, 1993.

(38) Kohlraush, R. *Pogg. Ann. Phys.* **1954**, *91*, 179.

(39) Williams, G.; Watts, D. C. *Trans. Faraday Soc.* **1970**, *66*, 80.

(40) Giordano, R.; Maisano, G.; Teixeira, J. *J. Appl. Crystallogr.* **1997**, *30*, 761.

(41) Chen, S.-H.; Bendedouch, D. *Methods in Enzymology* **1986**, *130*, 79.

(42) Magazù, S.; Migliardo, P.; Musolino, A. M.; Sciortino, M. T. *J. Phys. Chem. B* **1997**, *101* (13), 2348.

(43) Cazabat, A. M.; Langevin, D. *J. Chem. Phys.* **1981,** *74*, 3148.

(44) Branca, C.; Faraone, A.; Magazù, S.; Maisano, G.; Migliardo, F.; Migliardo, P.; Villari, V. *Recent Res. Dev. Phys. Chem.* **1999**, *3*, 361.

(45) Branca, C.; Magazù, S.; Maisano, G.; Migliardo, P. *J. Chem. Phys.* **1999**, *111*, 281.